A R C H I V E S O F M E T A L L U R G Y A N D M A T E R I A L S
Volume 52 2007 Issue 1

M. RICHERT*, H. PETRYK**, S. STUPKIEWICZ**

GRAIN REFINEMENT IN AlMgSi ALLOY DURING CYCLIC EXTRUSION – COMPRESSION: EXPERIMENT AND MODELLING

ROZDROBNIENIE ZIARNA W STOPIE AlMgSi PODCZAS CYKLICZNEGO WYCISKANIA – ŚCISKAJĄCEGO: BADANIA I MODELOWANIE

The effect of severe plastic deformation (SPD) during cyclic extrusion-compression (CEC) on grain refinement and strain hardening in AlMgSi alloy is studied quantitatively. New experimental results are presented showing that the average microband thickness and grain size decrease below 100 nm, i.e. a nanocrystalline material is obtained. In the modelling part, the decrease in size of dislocation cells and microbands is expressed in terms of the effective plastic strain defined such that strain rate reversals slow down its accumulation. Examples of simulation of the behaviour of AlMgSi alloy severely deformed by cyclic extrusion-compression are calculated and compared to experimental data.

Keywords: Modelling, Microstructure, Hardening, Severe plastic deformation

W pracy przeprowadzono ilościową analizę wpływu dużych deformacji plastycznych w procesie cyklicznego wyciskania ściskającego (CWS) na rozdrobnienie mikrostruktury i umocnienie plastyczne w stopie AlMgSi. Przedstawiono wyniki eksperymentalne pokazujące, że uzyskano strukturę nanokrystaliczną o średniej grubości mikropasm i wielkości ziarn poniżej 100 nm. W części dotyczącej modelowania, ewolucję mikrostruktury opisano przy użyciu efektywnego odkształcenia plastycznego, którego akumulacja jest spowolniona wskutek zmian kierunku prędkości odkształcenia na odwrotny. Przeprowadzono symulacje numeryczne zachowania się stopu AlMgSi w procesie CWS oraz porównano uzyskane wyniki z danymi doświadczalnymi.

1. Introduction

Cyclic extrusion-compression (CEC) [1] is one of the methods of applying severe plastic deformation (SPD) to polycrystalline materials in order to refine the grain size up to the submicrometer or nanometer level and, in consequence, to obtain extreme mechanical properties of the material. Other widely applied SPD methods include equal-channel angular pressing (ECAP) [2], high-pressure torsion (HPT) [3], multi-axis compression, and others. Unlike traditional cold rolling or drawing processes of large plastic deformation, the SPD techniques that employ cyclic strain paths lead to an essentially unchanged shape of the specimen after processing. The resulting microstructural and mechanical properties, for instance, the subgrain size, misorientation angle across boundaries, the fraction of the high angle boundary (HAGB) area and the flow stress or microhardness, have been measured in a number of papers, cf. [4, 5, 6, 7, 8, 9, 10].

Based on those extensive investigations, and also on certain ideas presented earlier in the literature, cf. [11, 12, 13, 14, 15, 16], a constitutive model of large-strain plasticity has recently been developed and used to simulate numerically the effect of applying different SPD routes for pure aluminium [17]. In the present paper, the model is applied to simulate the behaviour of AlMgSi aluminium alloy, and the results are compared to new experimental data.

2. Experimental results

Cyclic extrusion-compression (CEC) as the method of applying severe plastic deformation originated in 1979 [1]. The investigations started using a laboratory version of the CEC equipment. Recently, a new special hydraulic press with the control back-pressure has been designed and constructed, which is described in detail in Ref. [18]. A schematic illustration of the CEC process is shown in

* AGH UNIVERSITY OF SCIENCE AND TECHNOLOGY, 30-059 KRAKÓW, MICKIEWICZA 30, POLAND
** INSTITUTE OF FUNDAMENTAL TECHNOLOGICAL RESEARCH, POLISH ACADEMY OF SCIENCES, 00-049 WARSZAWA, ŚWIĘTOKRZYSKA 21, POLAND

Fig. 1. During plastic flow between two chambers of diameter d_0 through the connecting channel of diameter d_m, compression occurs simultaneously with extrusion, so that the sample is restored to its initial shape.

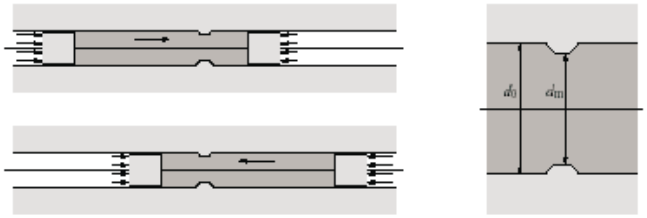

Fig. 1. A schematic illustration of the cyclic extrusion-compression process

In the work reported on here, AlMgSi samples were deformed using the new CEC press up to the accumulated equivalent von Mises strain (denoted frequently also by φ) $\varepsilon_{vM} = 16$. The samples were 10 mm in diameter and approximately 50 mm long. The channel diameter was $d_m = 8.5$ mm, which corresponds to a strain increment $\Delta\varepsilon_{vm} = 4 \ln(d_0/d_m) = 0.65$ exerted in a single CEC cycle.

TABLE 1
Measured average microband thickness D_b and average grain size D_g in AlMgSi after processing by CEC

No. of cycles	$\varepsilon_{\mathrm{vM}}$	D_b [nm]	D_g [nm]
3	1.95	187.1	257.9
7	4.55	132.3	219.1
15	9.75	100.4	138.7
25	16.25	77.5	70.8

AlMgSi (6082) is an alloy from the 6000 series. Its chemical composition is: Mg-1.15; Si-1.25; Mn-0.66; Fe-0.17; Cu-0.02; Zn-0.03; Ti-0,02; Cr-0.01 and Al. The 6082 alloy belongs to easy deformable materials which could be hardened by artificial ageing. The CEC deformation was performed at supersaturated state.

The microstructural investigations were performed on the longitudinal sections. The microstructure was investigated on thin foils using transmission electron microscope JEOL 2010 ARP. The special software KILIN [19] was used to determine disorientation on the base of the Kikuchi diffraction patterns.

The investigations of microstructure revealed the characteristic evolution from the ultrafine grained material at lower deformation to a nanomaterial at the deformation of $\varepsilon_{\mathrm{vm}} = 16$. The average intercept distance was measured in the direction orthogonal to microband boundaries, and in two orthogonal directions for grains. In Table 1, the decrease of the average microband thickness (D_b) in AlMgSi alloy with the increase of deformation is compared with the reduction of the mean size of grains (D_g). At the strain $\varepsilon_{\mathrm{vm}} = 16$ about 74% of the sample volume was occupied by the grains with the dimension below 100 nm.

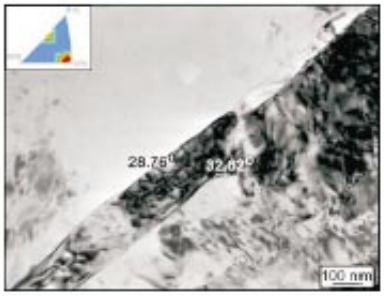

Fig. 2. Highly misoriented microbands in AlMgSi after the equivalent strain $\varepsilon_{\mathrm{vm}} = 10.5$; the microtexture is shown at the basic triangle

The investigations indicate that the mutual crossing of microbands can be a mechanism of formation of nanovolumes. The microbands in the material deformed to very large strains have highly-misoriented boundaries and are of the thickness below 100 nm (Fig. 2).

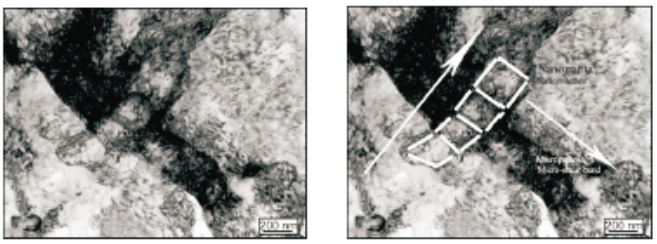

Fig. 3. The geometrical mechanism of creation of nanograins ($\varepsilon_{\mathrm{vm}} = 4.6$)

Mutual crossing of such microbands can facilitate the nanograin formation in a geometrical way (Fig. 3).

3. Modelling

3.1. The effective strain

Cyclic SPD processes like CEC or ECAP employ strain-rate reversals, either full or partial. It is well known that during cyclic plastic straining of a suffcient-ly small magnitude, typical stress-strain diagrams exhibit a stabilized hysteresis loop, i.e., saturation of isotropic work-hardening [20]. This can be attributed to the suspension of dislocation multiplication upon a strain-rate reversal until the process of transformation of dislocation cell walls during reverse activation of slip systems is completed. If the cyclic strain amplitude is larger then the suspension period is shorter than a half-cycle, nevertheless the resulting effectiveness of grain refinement versus the accumulated (equivalent or von Mises) plastic

strain ε_{vM} is expected to be slowed down in comparison to monotonic deformation.

To take this effect into account, the *effective* plastic strain, ε_{eff}, is introduced [17], whose rate is defined by

$$\dot{\varepsilon}_{eff} = \begin{cases} \dot{\varepsilon}_{vM} & \text{if } \mathbf{d}^p \cdot \mathbf{e}_r > 0 \quad \text{and } \|\mathbf{e}_r\| > r \\ 0 & \text{otherwise.} \end{cases} \tag{1}$$

It follows that $\dot{\varepsilon}_{eff}$ vanishes in a transitory process after a strain-rate reversal until the two inequality conditions in (1) are met again. They mean, first, that the plastic strain-rate $\mathbf{d}^p$ does not oppose a prestrain tensor $\mathbf{e}^r$ defined below, and second, that the magnitude of $\mathbf{e}^r$ exceeds a the threshold value r, which has been proposed in the form $r = r^\infty(1 - e^{-\varepsilon_{eff}/\varepsilon_r})$. The asymptotic value r^∞ of r strongly influences the ratio $\varepsilon_{eff}/\varepsilon_{vM}$ calculated for a given cyclic SPD process. For monotonic deformation, $\dot{\varepsilon}_{eff} = \dot{\varepsilon}_{vM} = \sqrt{\frac{2}{3}}\,\|\mathbf{d}^p\|$.

The prestrain tensor $\mathbf{e}^r$ is defined incrementally as follows

$$\overset{\nabla}{\mathbf{e}}_r = \mathbf{d}^p - \mathbf{e}_r \left\|\mathbf{d}^p\right\|/\varepsilon_r, \qquad \overset{\nabla}{\mathbf{e}}_r = \dot{\mathbf{e}}_r + \mathbf{e}_r\mathbf{w} - \mathbf{w}\mathbf{e}_r, \tag{2}$$

where $\dot{\mathbf{e}}_r$ is the material time derivative of $\mathbf{e}_r$, $\mathbf{w}$ the material spin, $\overset{\nabla}{\mathbf{e}}_r$ the corotational (Zaremba-Jaumann) rate of $\mathbf{e}_r$, and ε_r a material parameter. The term $(-\mathbf{e}_r\,\|\mathbf{d}^p\|/\varepsilon_r)$ restricts $\mathbf{e}_r$ to a recent prestrain.

The effective strain ε_{eff} is shown in Fig. 4 as a function of the equivalent von Mises strain ε_{vM} for several SPD processes: cyclic extrusion-compression (CEC) for two values 10:8 and 10:8.5 of the diameter ratio, equal-channel angular pressing (ECAP) for routes C and B_C with 90° die angle, and high pressure torsion (HPT). In each case, an idealized local deformation path is examined that corresponds to the given, most simple kinematics of plastic flow. No attempt is made here to study the effect of non-uniform deformation fields, e.g. of shear banding. The diagrams in Fig. 4 are defined it terms of two parameters, $r^\infty = 0.15$ and $\varepsilon_r = 0.2$. In case of HPT, ε_{eff} is simply equal to ε_{vM} as it is for rolling. Since CEC is a cyclic process with a relatively small amplitude, a much slower accumulation of ε_{eff} occurs, while the ECAP routes are in between.

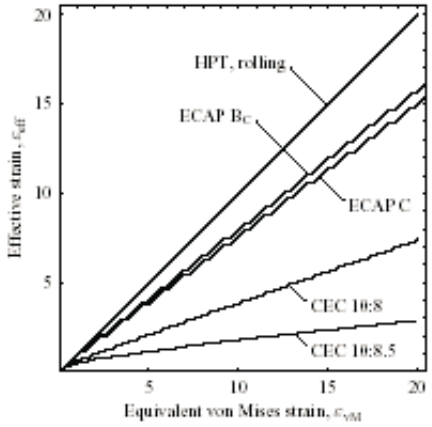

Fig. 4. Effective strain ε_{eff} as a function of the equivalent von Mises strain ε_{vM} for different SPD routes; $r^\infty = 0.15$, $\varepsilon_r = 0.2$

3.2. Evolution equations for microstructural parameters

A simplified microstructure created during plastic deformation is considered where equiaxed ordinary dislocation cells are placed between parallel boundaries of cell blocks or microbands, Fig. 5. D_c denotes the usual mean diameter of ordinary dislocation cells and D_b is the mean spacing between parallel cell-block boundaries. If the effective plastic strain becomes suffciently large then these dimensions are assumed to decrease to an asymptotic value. Simple formulae are proposed for describing such behaviour [17], namely

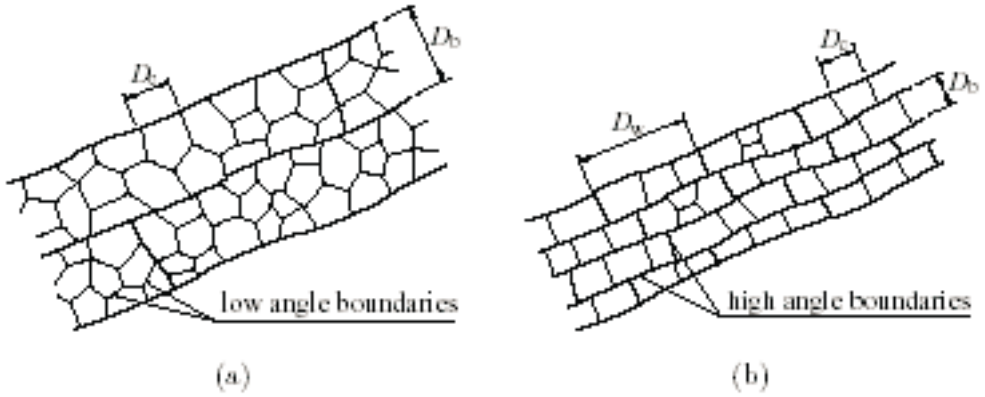

Fig. 5. Schematic view of microstructure created during plastic deformation at moderate (a) and large (b) strain

$$1/D_{\rm c} = 1/D_{\rm c}^{\infty} + (1/D_{\rm c}^{0} - 1/D_{\rm c}^{\infty})\exp(-\varepsilon_{\rm eff}/\varepsilon_{\rm c}) \qquad (3)$$

$$1/D_{\rm b} = 1/D_{\rm b}^{\infty} + (1/D_{\rm b}^{0} - 1/D_{\rm b}^{\infty})\exp(-\varepsilon_{\rm eff}/\varepsilon_{\rm b}). \qquad (4)$$

Each equation involves three parameters. $D_{\rm c}^{0}$ and $D_{\rm c}^{\infty}$ are the initial and the asymptotic cell size, respectively, and $\varepsilon_{\rm c}$ defines how fast $D_{\rm c}$ is evolving; the parameters in the expression for $D_{\rm b}$ have analogous meaning.

An important parameter in the description of microstructure evolution is the area fraction of high-angle boundaries (HAGB). At large strains examined here, a simplification is introduced that mean HAGB spacing in the directions normal and parallel to microbands is equal to $D_{\rm b}$ and $D_{\rm w}$, respectively, cf. thick lines in Fig. 5, while the remaining cell boundaries illustrated in Fig. 5 by thin lines correspond to low-angle misorientation. For the assumed simplified geometry of the microstructure, from purely geometric reasoning (e.g., for regular cubic cells), the high-angle boundary area fraction $\xi_{\rm h}$ can be roughly estimated from the formula

$$\xi_{\rm h} \approx D_{\rm c}(1/D_{\rm b} + 2/D_{\rm w})/3, \qquad (5)$$

The HAGB area fraction apparently saturates at very large deformation at a certain value $\xi_{\rm h}^{\infty} < 1$ [7, 8, 9]. If formula (5) is adopted then $\xi_{\rm h}^{\infty}$ corresponds to a saturation value $D_{\rm w}^{\infty} > D_{\rm c}^{\infty}$ for $D_{\rm w}$. $D_{\rm w}^{\infty}$ is expected to be approached faster for complex deformation paths, such that the newly created cell-block boundaries intersect older ones, cf. [21, 22]. Accordingly, a differential equation for $D_{\rm w}$ has been postulated in [17] that takes this effect into account. For cyclic extrusion-compression, we take a simpler version of that equation in the integrated form:

$$D_{\rm w} = D_{\rm w}^{\infty} + (D_{\rm w}^{0} - D_{\rm w}^{\infty})\exp(-\varepsilon_{\rm eff}/\varepsilon_{\rm w}), \qquad (6)$$

with three parameters of a similar meaning as in the equations for D_c and D_b.

Figure 6 shows the graphs that illustrate analytic expressions (3) and (4) calculated for CEC for the diameter ratio 10:8.5. The parameters $D_b^0 = 10$ μm, $D_b^{\infty} = 70$ nm and $\varepsilon_b = 1.4$ have been chosen to fit the experimental data for D_b given in Table 1 and marked in Fig. 6. The respective parameters for calculations of D_c and D_w have been taken more arbitrarily as $D_c^0 = 1.5$ μm, $D_c^{\infty} = 70$ nm, $\varepsilon_c = 0.3$, $D_w^0 = 25$ μm, $D_w^{\infty} = 100$ nm and $\varepsilon_w = 1.7$. The measured grain size D_g, marked in Fig. 6, lies between distant lines corresponding to D_c and D_w; the latter lies much higher that the range shown in Fig. 6.

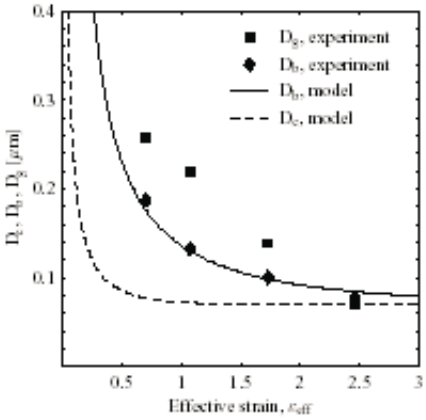

Fig. 6. Average cell size D_c and spacing of cell-block boundaries D_b versus the effective strain $\varepsilon_{\rm eff}$, calculated for CEC. The experimental data points correspond to the measured values given in Table 1

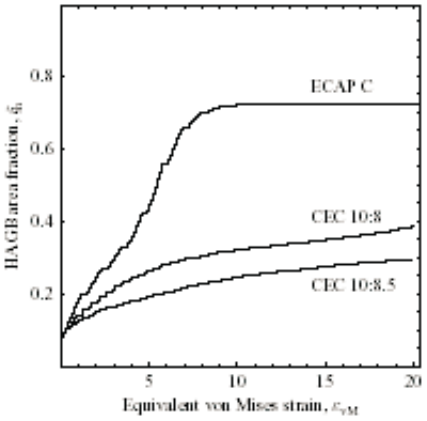

Fig. 7. High-angle boundary fraction $\xi_{\rm h}$ as a function of the equivalent von Mises strain $\varepsilon_{\rm vM}$ for three cyclic SPD routes

The evolution of the HAGB area fraction, estimated from formula (5), is shown in Fig. 7 versus the equivalent von Mises strain for the CEC process for two values, 10:8 and 10:8.5, of the diameter ratio. The HAGB area fraction during CEC grows more slowly than during the equal-channel angular pressing (ECAP) with route C, as illustrated in Fig. 7. This is due to relatively slower accumulation of the effective plastic strain $\varepsilon_{\rm eff}$ during CEC which corresponds to a lower cyclic strain amplitude than during ECAP with the 90° die angle.

3.3. Yield stress

With reference to a microstructure of the type visualized in Fig. 5, it has been proposed [11, 13] to determine the flow stress as the sum of the cell-block (or high-angle) boundary strengthening, expressed by a Hall-Petch relationship, and the dislocation strengthening, expressed by a term proportional to the square root

of the density of dislocations between high-angle boundaries. We shall use an alternative expression [17], viz.

$$\sigma_{\mathrm{y}} = \sigma_1 + (1-\xi_{\mathrm{h}})k_{\mathrm{c}}Gb\frac{1}{D_{\mathrm{c}}} + \xi_{\mathrm{h}}k_{\mathrm{b}}\frac{1}{\sqrt{D_{\mathrm{b}}}}. \qquad (7)$$

The first term σ_1 can be interpreted as a frictional stress. The second term, with G the elastic shear modulus and b the magnitude of the Burgers vector, represents the contribution from dislocations in low-angle boundaries (of average spacing D_c) and from dislocations between boundaries. The last term represents the contribution from higangle boundaries, primarily from parallel cell-block boundaries (of average spacing D_b). The coeffcients k_c and k_b are treated as material constants, while the leading factors $(1 - \xi_{\mathrm{h}})$ and ξ_{h} (the HAGB area fraction) are varying with the effective plastic strain.

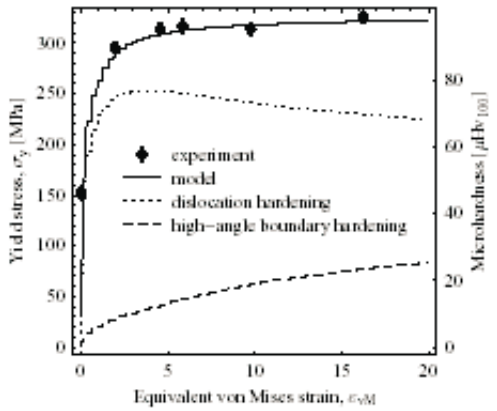

Fig. 8. Yield stress σ_y (solid line) and its contributions (dotted and dashed lines) as a function of the equivalent von Mises strain $\varepsilon_{\mathrm{vM}}$

The calculated yield stress evolution during processing by CEC with diameter ratio 10:8.5 is shown in Fig. 8 as a solid line. Typical values of G = 26 GPa and b = 0.286 nm have been adopted, while parameters k_{c} = 3 and k_{b} = 80 MPa μm$^{1/2}$ have been adjusted so that the calculated curve matches the experimental data points obtained from microhardness measurements, cf. Section 2. The dotted and dashed lines show the contributions to the total (isotropic) yield stress from the dislocation and high-angle boundary hardening, i.e. from the second and the third term in formula (7), respectively. The visible reduction of the former contribution at large plastic strains is related to the reduction of the factor $(1 - \xi_{\mathrm{h}})$, and not necessarily to any physical softening of the material.

4. Discussion and conclusion

The experimental results presented above show that CEC as a method of applying severe plastic deformation without affecting the initial shape of the material sample is capable of refining the grain size in AlMgSi alloy below 100 nm. A geometrical mechanism of creation of nanograins by mutual crossing of microbands is inferred.

A quantitative description of grain subdivision and strain hardening during CEC has been obtained by applying a new, physically motivated constitutive model. The effective plastic strain $\varepsilon_{\mathrm{eff}}$ is introduced whose growth is suspended for a transitory period after a strain rate reversal. Dislocation cell size and cell-block thickness are modelled as functions of $\varepsilon_{\mathrm{eff}}$. Since CEC is a cyclic process with a relatively small amplitude, a slower grain refinement than during ECAP is predicted for comparable values of the equivalent strain $\varepsilon_{\mathrm{vM}}$, at least when nominal deformation paths (without shear banding) are only compared.

Evolution of the flow stress during large plastic deformation is described by incorporating the strain hardening due to both dislocation and boundary strengthening. The respective additive terms enter the proposed formula for the flow stress with variable weighting factors equal to the estimated area fractions of low and high angle boundaries. In effect, saturation of the flow stress need not correspond to reaching a steady state but can be accompanied by further evolution of the microstructure towards an equiaxed subgrain structure.

Acknowledgements

This work has been supported by the State Committee for Scientific Research (KBN) in Poland through Grant No. PBZ-KBN-096/T08/2003.

REFERENCES

[1] J. Richert, M. Richert, A new method for unlimited deformation of metals and alloys. Aluminium **62(8)**, 604-607, 1986.

[2] V.M. Segal, Materials processing by simple shear. Mater. Sci. Eng. A **197**, 157-164, 1995.

[3] R.Z. Valiev, Y.V. Ivanisenko, E.F. Rauch, B. Baudelet, Structure and deformation behaviour of Armco iron subjected to severe plastic deformation. Acta Mater. **44(12)**, 4705-4712, 1996.

[4] Y. Iwahashi, Z. Horita, M. Nemoto, T.G. Langdon, An investigation of microstructural evolution during equal-channel angular pressing. Acta Mater. **45(11)**, 4733-4741, 1997.

[5] Y. Iwahashi, Z. Horita, M. Nemoto, T.G. Langdon, Factors influencing the equilibrium grain size in equal-channel angular pressing: Role of Mg additions to aluminum. Metall. Mater. Trans. A **29(10)**, 2503-2510, 1998.

[6] M. Richert, Q. Liu, N. Hansen, Microstructural evolution over a large strain range in aluminium deformed

by cyclic-extrusion-compression. Mater. Sci. Eng. A **260**, 275-283, 1999.

[7] M. Richert, J. Richert, S. Hawryłkiewicz, A. Wusatowska, Microstructure of heavily deformed materials. Inżynieria Materiałowa **5**, 776-779, 2001.

[8] S.D. Terhune, D.L. Swisher, K. Oh-ishi, T.G. Langdon, T.R. McNelley, An investigation of microstructure and grain-boundary evolution during ECA pressing of pure aluminum. Metall. Mater. Trans. A **33**, 2173-2184, 2002.

[9] P.B. Prangnell, J.R. Bowen, P.J. Apps, Ultra-fine grain structures in aluminium alloys by severe deformation processing. Mater. Sci. Eng. A **375-377**, 178-185, 2004.

[10] K. Furuno, H. Akamatsu, K. Oh-ishi, M. Furukawa, Z. Horita, T.G. Langdon, Microstructural development in equal-channel angular pressing using a 60° die. Acta Mater. **52**, 2497-2507, 2004.

[11] D.A. Hughes, N. Hansen, Microstructure and strength of nickel at large strains. Acta Mater. **48**, 2985-3004, 2000.

[12] Y. Estrin, L.S. Toth, A. Molinari, Y. Brechet, A dislocation-based model for all hardening stages in large strain deformation. Acta Mater. **46(15)**, 5509-5522, 1998.

[13] N. Hansen, X. Huang, D.A. Hughes, Microstructural evolution and hardening parameters. Mater. Sci. Eng. A **317**, 3-11, 2001.

[14] B. Peeters, M. Seefeldt, C. Teodosiu, S.R. Kalidindi, P. van Houtte, E. Aernoudt, Work-hardening/softening behaviour of b.c.c. polycrystals during changing strain paths: I. An integrated model based on substructure and texture evolution, and its prediction of stress-strain behaviour of an IF steel during two-stage strain paths. Acta Mater. **49**, 1607-1619, 2001.

[15] R. Sedlacek, W. Blum, J. Kratochvil, S. Forest, Subgrain formation during deformation: physical origin and consequences. Metall. Mater. Trans. A **33**, 319-327, 2002.

[16] U.F. Kocks, H. Mecking, Physics and phenomenology of strain hardening: the FCC case. Progress Mater. Sci. **48**, 171-273, 2003.

[17] H. Petryk, S. Stupkiewicz, A quantitative model of grain refinement and strain hardening during severe plastic deformation. Mater. Sci. Eng. A, 2006. doi:10.1016/j.msea.2006.08.076 (in print).

[18] J. Richert, Strain-stress conditions of shear band formation during CEC processing on a new machine with control of back-pressure. J. Mat. Proc. Technol. (in print).

[19] M. Richert, K. Chruściel, A. Baczmański, J. Długopolski, Mikroanaliza II – Dezorientacje i Mikrostruktura KILIN 1.21. Kraków, 2002.

[20] J.-L. Chaboche, Time independent constitutive theories for cyclic plasticity. Int. J. Plasticity **2**, 149-188, 1986.

[21] M. Furukawa, Z. Horita, T.G. Langdon, Factors influencing the shearing patterns in equal-channel angular pressing. Mater. Sci. Eng. A **332**, 97-109, 2002.

[22] C. Xu, M. Furukawa, Z. Horita, T.G. Langdon, The evolution of homogeneity and grain refinement during equal-channel angular pressing: A model for grain refinement in ECAP. Mater. Sci. Eng. A **398**, 66-76, 2005.

Received: 20 October 2006.